

# Impact of Background Processes in the $H \rightarrow Z\gamma$ Decay

Aliaksei Kachanovich  
Université libre de Bruxelles  
May 21, 2025

IRN Terascale in Strasbourg

ULB

## 1 Motivation

## 2 Theory

- The SM
- The NP contribution

## 3 Phenomenology

- Resonant contribution rescaling vs. new background
- Phenomenological constraints

## 4 Conclusion



# Motivation

# Motivation

- Rare Standard Model (SM) processes may shed light on open questions, such as dark matter, baryon asymmetry, and neutrino masses.
- The decay  $H \rightarrow Z\gamma$  is a rare process within the SM.
- ATLAS and CMS reported a branching fraction of  $(3.4 \pm 1.1) \times 10^{-3}$  for  $H \rightarrow Z\gamma$  process, which is higher by a factor of  $2.2 \pm 0.7$  compared to the SM prediction.
- The excess has been interpreted as a modification of the  $HZ\gamma$  vertex.
- Detectors measure  $H \rightarrow \ell\ell\gamma$ ; excess events may also be due to new physics (NP) backgrounds.

The content of this talk closely follows the analysis in [\[arXiv:2503.08659\]](#), in collaboration with J. Kimus (ULB), S. Lowette (VUB, IIHE), and M.H.G. Tytgat (ULB).



# Motivation

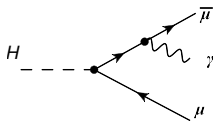
- EFT and UV-complete models responsible for the branching fraction of  $(3.4 \pm 1.1) \times 10^{-3}$  for  $H \rightarrow Z\gamma$ .
- Methods to falsify background scenarios.
- Constraints on our models from other observed phenomena.

The content of this talk closely follows the analysis in [\[arXiv:2503.08659\]](https://arxiv.org/abs/2503.08659), in collaboration with J. Kimus (ULB), S. Lowette (VUB, IIHE), and M.H.G. Tytgat (ULB).

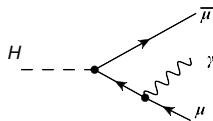


# Theory

# Theory. The SM

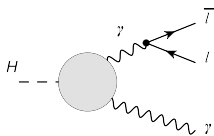


(a)

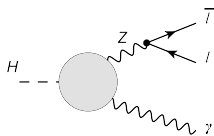


(b)

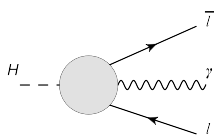
Tree-level amplitude. Due to the small electron Yukawa coupling, this contribution is relevant only for the dimuon channel.



(c)



(d)



(e)

Loop amplitudes (schematic) contributing to  $H \rightarrow l\bar{l}\gamma$ .

# Theory. The SM

- The one-loop amplitude can be expressed as [\[arXiv:2001.06516\]](#)

$$\mathcal{M}_{\text{SM,loop}} = [(q_\mu p_{1\nu} - g_{\mu\nu} q \cdot p_1) \bar{u}(p_2) (A_1 \gamma^\mu P_R + B_1 \gamma^\mu P_L) v(p_1) + (q_\mu p_{2\nu} - g_{\mu\nu} q \cdot p_2) \bar{u}(p_2) (A_2 \gamma^\mu P_R + B_2 \gamma^\mu P_L) v(p_1)] \varepsilon^{*\nu}(q),$$

- Tree level

$$\mathcal{M}_{\text{SM, tree}} = -\frac{e^2 m_\mu \varepsilon_\nu^*(q)}{2m_W \sin \theta_W} \times \left[ \frac{\bar{u}(p_1)(\gamma^\nu \not{q} + 2p_1^\nu) v(p_2)}{t - m_\ell^2} - \frac{\bar{u}(p_1)(\gamma^\nu \not{q} + 2p_2^\nu) v(p_2)}{u - m_\ell^2} \right].$$

# Theory. The NP contribution

- On the level of effective field theory, the contribution to the  $ll\gamma$  background is described by a dimension-8 effective operator [\[arXiv:1008.4884\]](#)

$$\mathcal{L}_{\text{eff}} \supset \frac{g'}{\Lambda_R^4} |H|^2 \partial_\nu (\bar{\ell}_R \gamma_\mu \ell_R) B^{\mu\nu}.$$

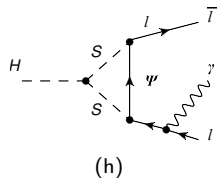
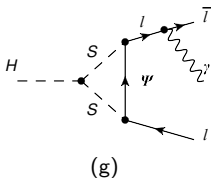
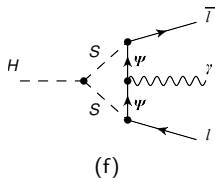
- Other effective operators also contribute to the  $H \rightarrow ll\gamma$  process.

# Theory. The NP contribution

- One of possible UV-complete solution which can provide missing events described by the Dark matter model [\[arXiv:1405.6921\]](#)

$$\mathcal{L} \supset \frac{1}{2} \partial_\mu S \partial^\mu S - \frac{1}{2} m_S^2 S^2 + \bar{\Psi} (i \not{D} - m_\Psi) \Psi - \sum_\ell (y_\ell S \bar{\Psi} \ell_R + h.c.) - \frac{\lambda_{hs}}{2} S^2 |H|^2$$

- This Lagrangian gives rise to three new Feynman diagrams contributing to  $H \rightarrow \ell \ell \gamma$





# Phenomenology

# Phenomenology

## General overview

- The experimental branching fraction can be obtained for the scale  $\Lambda_R = 246$  GeV.
- In the UV-complete theory, there are 4 new parameters that impact the decay rate.
- One solution can be at  $m_\Psi = m_S = 62.5$  GeV with the  $\ell S \Psi$  vertex coupling  $y_\ell = 1.66$  and  $HSS$  vertex coupling  $y_{hs} = 0.26$ .
- Another scenario:  $m_\Psi = m_S = 100$  GeV with  $y_\ell^2 \cdot y_{hs} = 28.1$ .



# Phenomenology

## Definition of resonant contribution

- The loop contribution consists of resonant and non-resonant parts  
[arXiv:2109.04426]:

$$a_{1(2)}(s, t) = a_{1(2)}^{nr} + a_{1(2)}^{res}(s),$$

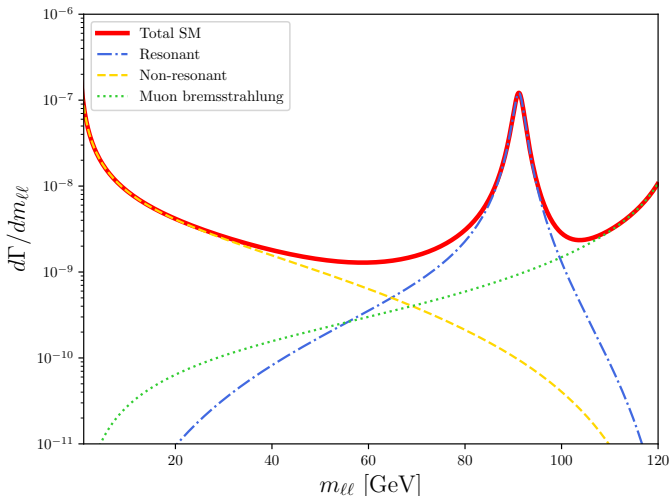
where

$$a_{1(2)}^{nr} \equiv \tilde{a}_{1(2)}(s, t) + \frac{\alpha(s) - \alpha(m_Z^2)}{s - m_Z^2 + im_Z\Gamma_Z}, \quad a_{1(2)}^{res}(s) \equiv \frac{\alpha(m_Z^2)}{s - m_Z^2 + im_Z\Gamma_Z}.$$

# Phenomenology

## SM contribution to $H \rightarrow \ell\bar{\ell}\gamma$

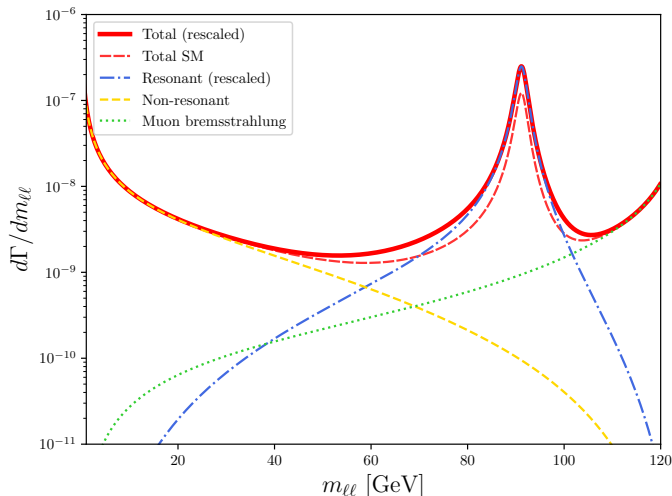
- The resonant contribution corresponds to the process  $H \rightarrow Z\gamma$ , while the non-resonant contribution includes box diagrams and  $H \rightarrow \gamma\gamma$ .



# Phenomenology

## Contribution with rescaled resonant part

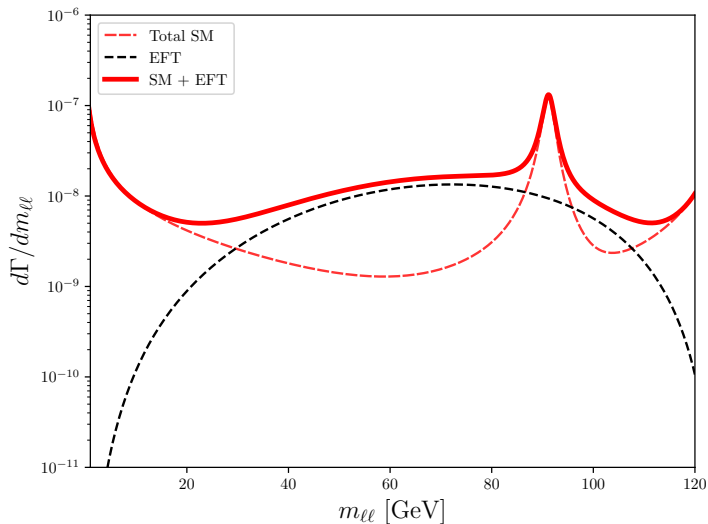
- To simulate the differential decay rate from the experiment, we rescale the resonant contribution in the process  $H \rightarrow \ell\ell\gamma$ .



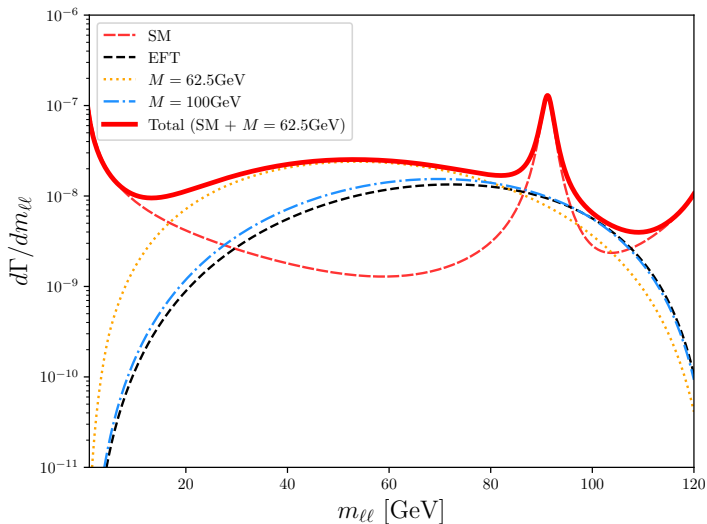
# Phenomenology

## Effective operator

The differential decay rate with the contribution of the effective operator.



The differential decay rate with the contribution of the UV-complete theory.



# Phenomenology

## Kinematical cuts impact

Theoretical decay rates and the experiment-to-theory ratio for a typical choice of cuts.

#	Cuts	$m_{\ell\ell}^{\min}$	$m_{\ell\ell}^{\max}$	$\Gamma_{\text{tot}}^{\text{SM}}$	$\Gamma_{\text{tree}}^{\text{SM}}$	$\frac{Br_{\text{resc}}}{Br_{\text{SM}}}$	$\frac{Br_{\text{EFT}}}{Br_{\text{SM}}}$	$\frac{Br_{\text{UV}}}{Br_{\text{SM}}}$
1	None	50	125	0.768	0.287	1.67	1.86	2.07
2	None	50	100	0.504	0.028	2.01	2.21	2.57
3	CMS	40	125	0.455	0.011	2.04	2.10	2.13
<b>4</b>	<b>CMS</b>	<b>50</b>	<b>125</b>	<b>0.451</b>	<b>0.011</b>	<b>2.06</b>	<b>2.06</b>	<b>2.06</b>
5	CMS	70	125	0.440	0.011	2.07	1.80	1.71
6	CMS	70	100	0.432	0.006	2.08	1.74	1.68
7	CMS	80	100	0.416	0.005	2.09	1.48	1.39

**Table:** CMS cuts:  $E_\gamma \geq 15$  GeV,  $E_1 \geq 7$  GeV,  $E_2 \geq 25$  GeV and  $t_{\min}, u_{\min} \geq (0.1 m_H)^2$ .  $m_{\ell\ell}^{\min(\max)}$  are in GeV,  $\Gamma_{\text{tot}(\text{tree})}^{\text{SM}}$  are in keV. UV-complete theory:  $m_S = m_F = 62.5$  GeV.

# Phenomenological constraints

## Muon magnetic dipole moment

- Contribution to the muon's electromagnetic form factor  $F_2(q^2)$  with  $q$  photon momenta

$$\Delta F_2(0) \hat{=} \Delta \left( \frac{g_\mu - 2}{2} \right) \hat{=} \Delta a_\mu = \frac{y_\ell^2}{192\pi^2} \frac{m_\mu^2}{M^2}$$

is positive.

- For  $y_\ell = 1.28$  and  $m_S = 62.5$  GeV (corresponding to  $\lambda_{hs} y_\ell^2 = 0.72$  if  $\lambda_{hs} = 0.44$ ), is  $\Delta a_\mu = 2.5 \cdot 10^{-9}$ . A similar shift can be obtained with  $y_\ell = 2.05$ .
- For  $m_S = 100$  GeV, corresponding respectively to  $\lambda_{hs} y_\ell^2 = 28.1$  for  $\lambda_{hs} = 6.7$ .
- The Standard Model prediction for the muon anomalous magnetic moment is  $a_\mu(\text{exp}) - a_\mu(\text{SM}) = (251 \pm 59) \cdot 10^{-11}$ , that lies within the range of the UV model prediction.

# Phenomenological constraints

## Electroweak precision tests (EWPT)

- For  $m = m_S = 62.5(100)$  GeV

$$\left. \frac{\Delta\Gamma}{\Gamma} \right|_{\text{inv}} = 0.0002 (0.00005) < 0.003$$

$$\left. \frac{\Delta\Gamma}{\Gamma} \right|_{\ell\ell} = 0.0002 (0.00006) < 0.001$$

$$\Delta m_W = 0.0082 (0.0026) \text{ GeV} < 0.013 \text{ GeV}$$

- Oblique corrections are significantly smaller than the current  $1\sigma$  experimental uncertainties.



# Phenomenological constraints

## Constraints from colliders

- Masses of  $\Psi$  and  $S$  are degenerate, with  $m_\Psi \gtrsim m_S$ .
- As the Yukawa coupling is not small, the process  $\Psi^{(-)} \rightarrow S + \ell^{(-)}$  leads to soft leptons, which escape detection. The production of  $\Psi\bar{\Psi}$  is thus equivalent to missing energy,  $pp \rightarrow \text{jets} + \cancel{E}$ .
- Collider detection limits can be estimated by comparing the processes  $q\bar{q} \rightarrow Z' \rightarrow \chi\bar{\chi}$  and  $q\bar{q} \rightarrow Z/\gamma \rightarrow \Psi\bar{\Psi}$ .
- Bound:  $m_F \gtrsim 67$  GeV (within 5%); benchmark with  $m_\Psi \gtrsim m_S = 62.5$  GeV is borderline, while  $m_\Psi \gtrsim m_S = 100$  GeV is safe.

# Phenomenological constraints

## Comments on DM direct detection

- In thermal freeze-out, the abundance  $Y_S = n_S/s$  (with  $s$  the entropy density) scales as  $Y_S \propto 1/\langle\sigma v\rangle \propto 1/\lambda_{hs}^2$ .
- For the benchmark  $S$  particle with mass  $m_S = 100$  GeV, thermal freeze-out requires a large quartic coupling:  $\lambda_{hs} \gtrsim 2.2$ .
- For  $S$  to account for all of DM ( $f_S = 1$ ), one would instead need  $\lambda_{hs} \approx 0.04$ .
- If stable, the  $S$  particle would therefore be a subdominant DM component:  $f_S \approx (0.04/2.2)^2 \approx 3 \cdot 10^{-4}$ .
- This benchmark is excluded by direct detection. A lighter  $S$  particle, with  $m_S$  slightly above  $m_H/2$ , may still evade direct detection due to proximity to the Higgs resonance.

# Conclusion

# Conclusion

- There is background from  $H \rightarrow \gamma\gamma$ , tree-level bremsstrahlung, and box diagrams, which is cut-dependent.
- Appropriate kinematics cuts substantially reduce the background.
- EFT provides a possible explanation for the enhanced decay rate at the scale  $\Lambda_R = 246$  GeV.
- There is a possible solution in terms of the UV-complete theory.
- The differential decay rate from the experiment is needed.
- Both the UV-complete model and EFT remain consistent with the current muon  $g - 2$  measurement, electroweak precision tests (EWPT), and collider measurements.
- Different kinematic cuts provide the possibility to constrain the model parameters.

The background of the slide is a dark, futuristic tunnel with concentric circular patterns on the walls and floor. A bright blue light source is at the end of the tunnel, with several blue and orange laser beams radiating from it. The text 'Merci beaucoup !' is displayed in a white rounded rectangle in the upper left area.

Merci beaucoup !